



Triangulene GQD as a Toxic Gas Sensor: A First Principle Study

Drashti Patel*, Rahul Prajapati**

** Assistant Professor, Science & Humanity Department, Hansaba College of Engineering & Technology, Gokul Global University, Sidhpur, Gujarat, India.

Abstract

In this work, we have investigated Graphene quantum dot “triangulene” using first principles based density functional theory (DFT) by means of adsorption mechanism and electronic density of states calculations. The computed adsorption energy of triangulene over NH_3 gas molecule is -0.177eV which shows minimum energetic configuration for NH_3 . Further, we have studied Ni doped triangulene for better adsorption mechanism. Three different sites on triangulene were considered for Ni atom adsorption namely top site of carbon (C) atom, hollow site of the hexagon carbon ring near triangulene unpaired electron and bridge site over C–C bond. We have calculated the density of states (DOS), highest occupied molecular orbitals (HOMO), lowest unoccupied molecular orbitals (LUMO) and HOMO-LUMO gap of Ni doped triangulene. Our result shows that Ni doped triangulene can be used as a remover purpose of CO and NH_3 from specific environments. Despite of the adsorption distance (2.24\AA), Ni-doped triangulene can be used for detection of CS_2 gas molecule due to the short recovery time.

DOI: 10.48047/ecb/2022.11.12.42

Introduction

Recently discovered zero-dimensional graphene quantum dots (GQDs) are new and arising members of graphene family [1] with sizes usually below 10 nm. GQDs acquire size-shape dependent bandgap and unique photoluminescence (PL) properties due to quantum confinement and edge effects. Moreover, they have low-toxicity, chemical inertness, biocompatibility, and no photo-bleaching properties, promoting their applications in many fields, including photo electronics and catalysis [2]. Further to achieve the full potential of GQDs, GQDs-based nanocomposites have been studied [3]. Various nanocomposites based on Nobel metals like aluminium, silver, platinum, Nickel, and palladium with GQDs were also studied. Cutting the graphene sheet leads to the several nano-fragments of graphene, in which one can see various structures of polycyclic aromatic hydrocarbons (PAHs) like anthracene, pyrene, coronene, triangulene, phenalenyl and ultimately benzene. In present work, we study the role of graphene quantum dots (GQD) towards the toxic gases. Quantum mechanical calculations based on density functional theory (DFT) were performed to study the adsorption mechanism and electronic properties of the aforementioned. We use open shell GQD, triangulene ($\text{C}_{22}\text{H}_{12}$) as a model system for adsorption. Furthermore, for adsorption, we investigated the site dependent adsorption mechanism of gas molecule over Ni doped triangulene. The bridge (B), hollow (H) and top (T) sites were considered for the adsorption of gas molecule to understand triangulene capacity for good adsorption performance.

Computational methodology

In this work, all the geometrical optimization, adsorption mechanism and electronic properties calculation were performed with the Gaussian 09 program. we have performed all the calculations using B3LYP (Becke three Lee Yang Perdew) hybrid function. The hybrid functionals are the mixture of Hartee-Fock (HF) and Density Functional theory (DFT). All geometry optimizations were performed using the 6-311 G (d, p) Gaussian basis set. Same level of theory has been adapted to calculate total energies, electronic parameters, density of states (DOS), global indices parameters, work function, relaxation time and adsorption energies. Visualizations of molecular orbitals are rendered with Gauss View (version 5) using the result of DFT calculation. The Nickel atom is modelled as being adsorbed at one of three different positions: (i)bridge site (ii) hollow site(iii) top site. Throughout the manuscript, all three sites were named as Tri+Ni(B) for bridge site, Tri+Ni(H) for Hollow site and Tri+Ni(T) for top site. The adsorption energy between the system was calculated by:

$$E_{ad} = E_{(Tri+gas)} - (E_{(Tri)} + E_{(gas)}) \dots\dots\dots (1)$$

$$E_{ad} = E_{(Tri+Ni+gas)} - (E_{(Tri+Ni)} + E_{(gas)}) \dots\dots\dots (2)$$

Where E_{Tri+Ni} is the optimized energy of system in which Nickel is absorbed on triangulene (on three different sites), E_{tri} is the optimized energy of pristine triangulene. With the definition, a negative E_{ad} value shows a stable adsorption complex on the triangulene. The energy bandgap (E_g) is calculated through the highest occupied molecular orbitals (HOMO) and lowest unoccupied molecular orbitals (LUMO). the expression for energy bandgap is given by,

$$E_g = E_{LUMO} - E_{HOMO} \dots\dots\dots (3)$$

Fermi level energy (E_F) (b) is given by following relation

$$E_f = (E_{LUMO} + E_{HOMO})/2 \dots\dots\dots (4)$$

To represent the gas electronic sensitivity of the pristine, the variation of the energy gap is calculated as:

$$\Delta E_g = [(E_{g2} - E_{g1})/E_{g1}] \times 100\% \dots\dots\dots (5)$$

Where E_{g1} and E_{g2} stand for the energy gaps of the pristine and complex, respectively.

RESULT AND DISCUSSION

• Structural and electronic properties of pristine Triangulene nanocluster:

Before proceeding to the study of adsorption performance of CO,CS₂,NH₃ hazardous gas molecules towards pristine triangulene ,we optimized the triangulene system with B3LYP hybrid function and 6-13 G(d,p) basis set .the ground state optimized geometry is represented in fig.1(a).the structural parameters are shown in table-1.the HOMO and LUMO energies are - 3.53eV and -3.47eV ,respectively and calculated E_G of triangulene pristine using eq(1) is 0.06eV .the calculated fermi energy level E_f eq(4) which is -3.50eV which lies in the middle of the HOMO and LUMO .the HOMO and LUMO electron densities are shown in fig -1(b , c) and ESP maps(see fig.1(d)) colour choice is arbitrary, red and green colour represents the

negative and positive isosurface, respectively. From ESP analysis we can identify which site of system is more suitable for adsorbing gas molecules. We analysed Mulliken charge population which clearly shows that the positive and negative charge distribution on adjacent carbon and hydrogen atoms respectively (see fig-1(e)). Figure -2 represent the density of state (DOS) plot of the triangulene pristine which corroborates the calculated value of HOMO, LUMO and E_G (see in table -1).

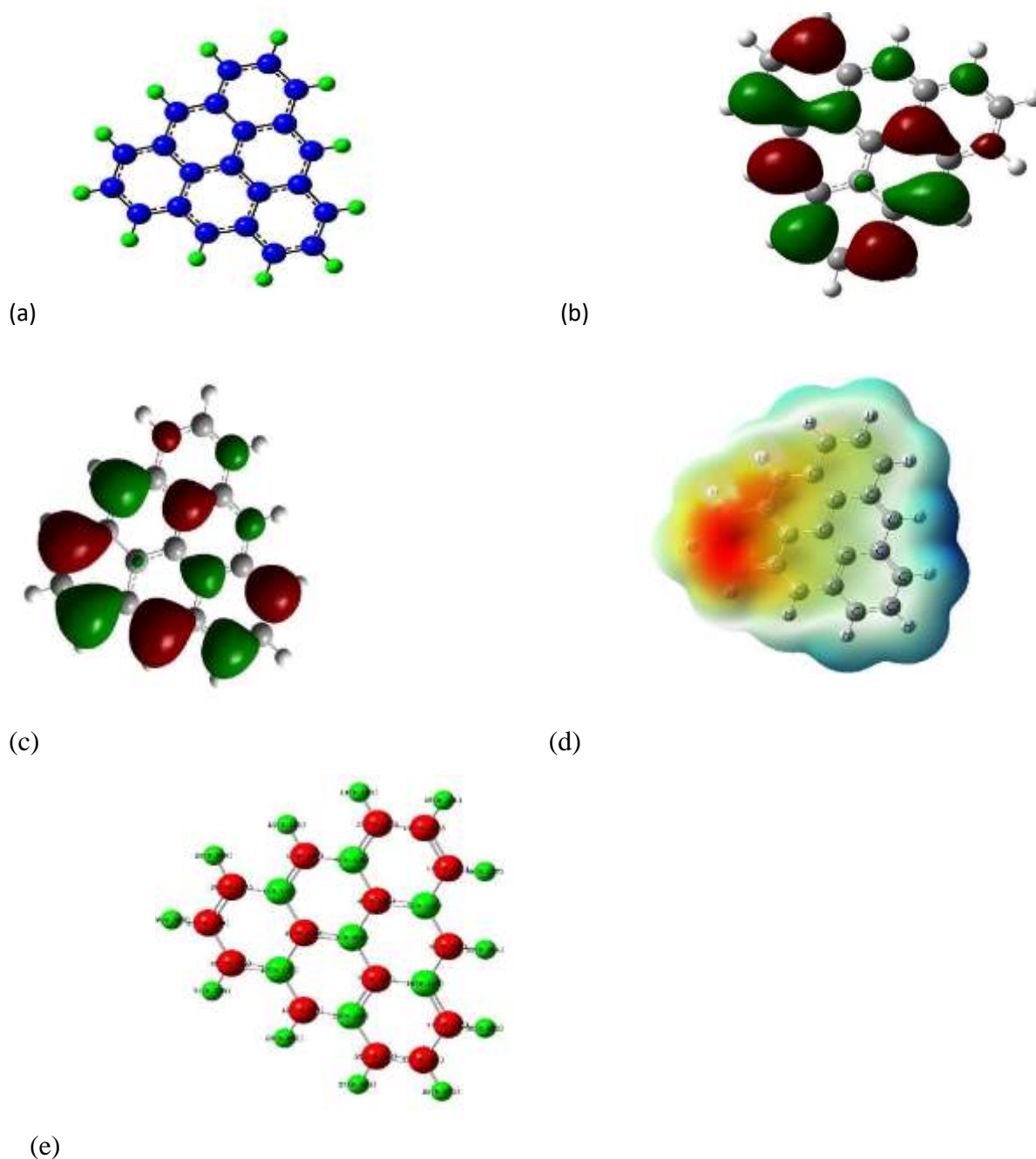


Figure 1. Optimized geometry (a), HOMO electron density (b), LUMO electron density (c), ESP(d) and Mulliken charge population analysis (e) of pristine triangulene, respectively

system	Bond Length(Å)	Bond Angle (°)	E _{HOMO} (eV)	E _{LUMO} (eV)	E _G (eV)	DIPOLE MOMENT (DEBYE)	Fermi Energy (eV)
Triangulene	1.41	119.65	-3.53	-3.47	0.06	4.63	-3.50

Table-1: Structural parameter, HOMO and LUMO energies (E_{HOMO} and E_{LUMO}), HOMO LUMO band gap (E_G) and dipole moment of triangulene.

To confirm the structural stability of triangulene pristine the formation of energy is calculated by the following formula

$$E = (1/34) [E(C_{22}H_{12}) - 22E(C) - 12E(H)] \text{-----(6)}$$

Where, E(C₂₂H₁₂) the energy of triangulene pristine, E(C) is the energy of the isolated carbon and E(H) is the energy of the isolated hydrogen atom, respectively. The formation energy of triangulene pristine is -6.84eV/atom. The negative value of the formation energy ensures the stability of the triangulene [4].

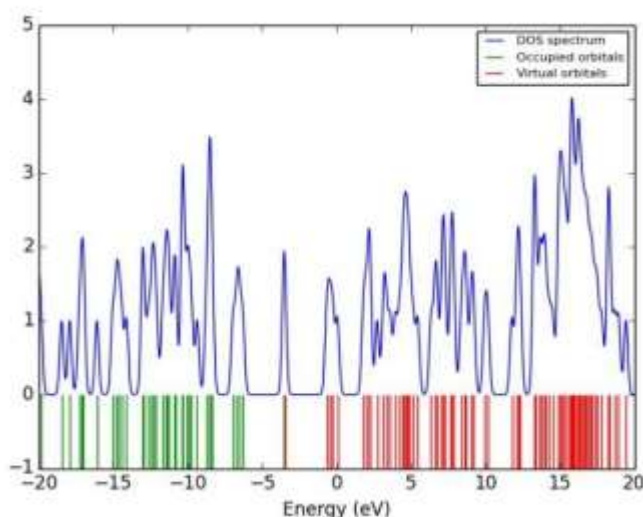


Figure 2. DOS spectra of pristine triangulene.

● Adsorption properties of CO, CS₂ and NH₃ gas molecules adsorbed triangulene nanocluster:

We optimized isolated hazardous gas molecule (CO, CS₂, NH₃) and analysed structural and vibrational properties of it. the interaction of gas molecule and triangulene can be understood by the adsorption energy (E_{ad}) and calculated using the following equation:

$$E_{ad} = E(C_{22}H_{12}+gas)-E(C_{22}H_{12}) - E(gas)\text{-----(7)}$$

Where, E(C₂₂H₁₂+gas), E(C₂₂H₁₂), E(gas) are the total energy gas adsorbed triangulene, total energy of pristine triangulene and total energy of isolated gas molecule respectively. we have adsorbed hazardous NH₃ and CS₂ gas molecule at various sites and various orientation of the gas molecules at each site of triangulene. for CO we have also considered different sites of CO at different sites of triangulene. out of several possibilities for each gas molecule, the most

stable configuration i.e., minimum energetic configuration is considered for the further calculation. The computed adsorption energy (using eq (2)) of NH_3 gas molecule over triangulene is -0.177eV . Figure-3(a) shows minimum energetic configuration for NH_3 adsorption. After NH_3 gas adsorption, the distance of the N head of NH_3 gas is 2.43\AA from nearest carbon atom of the triangulene. Minimum energetic configuration of CS_2 adsorption is shown in Figure-3(b) and adsorption energy of CS_2 adsorption over triangulene is 0.029eV . After CS_2 gas adsorption, the distance of C head of CS_2 gas is 2.24\AA . Figure-3(c) present the minimum energetic configuration of CO adsorption over triangulene depicts that the adsorption of CO gas molecules occurred at bridge site of triangulene with the adsorption energy is -0.0259eV . Nearest distance of the O atom of CO gas molecule from carbon atom of the triangulene is 3.36\AA as shown in Table 2.

System	$E_{\text{ads}}(\text{eV})$	$E_{\text{HOMO}}(\text{eV})$	$E_{\text{LUMO}}(\text{eV})$	$E_{\text{G}}(\text{eV})$	$E_{\text{f}}(\text{eV})$	$\Delta E_{\text{f}}(\text{eV})$	$\Delta E_{\text{g}}(\text{eV})$	$d(\text{\AA})$	DIPOLE MOMENT (DEBYE)
$\text{C}_{22}\text{H}_{12}\text{CO}$	-0.025	-3.57	-3.49	0.08	-3.53	-0.85%	+33.33%	3.36	4.99
$\text{C}_{22}\text{H}_{12}\text{CS}_2$	-0.029	-3.63	-3.54	0.09	-3.58	-2.28%	+50%	3.60	5.29
$\text{C}_{22}\text{H}_{12}\text{NH}_3$	-0.177	-3.34	-3.21	0.13	-3.27	+6.57%	+116.67%	2.43	7.47

Table 2: Adsorption energy (E_{ad}), HOMO energy (E_{HOMO}), LUMO energy (E_{LUMO}), HOMO – LUMO gap (E_{G}) and fermi energy (E) of CO , CS_2 and NH_3 gas adsorbed triangulene.

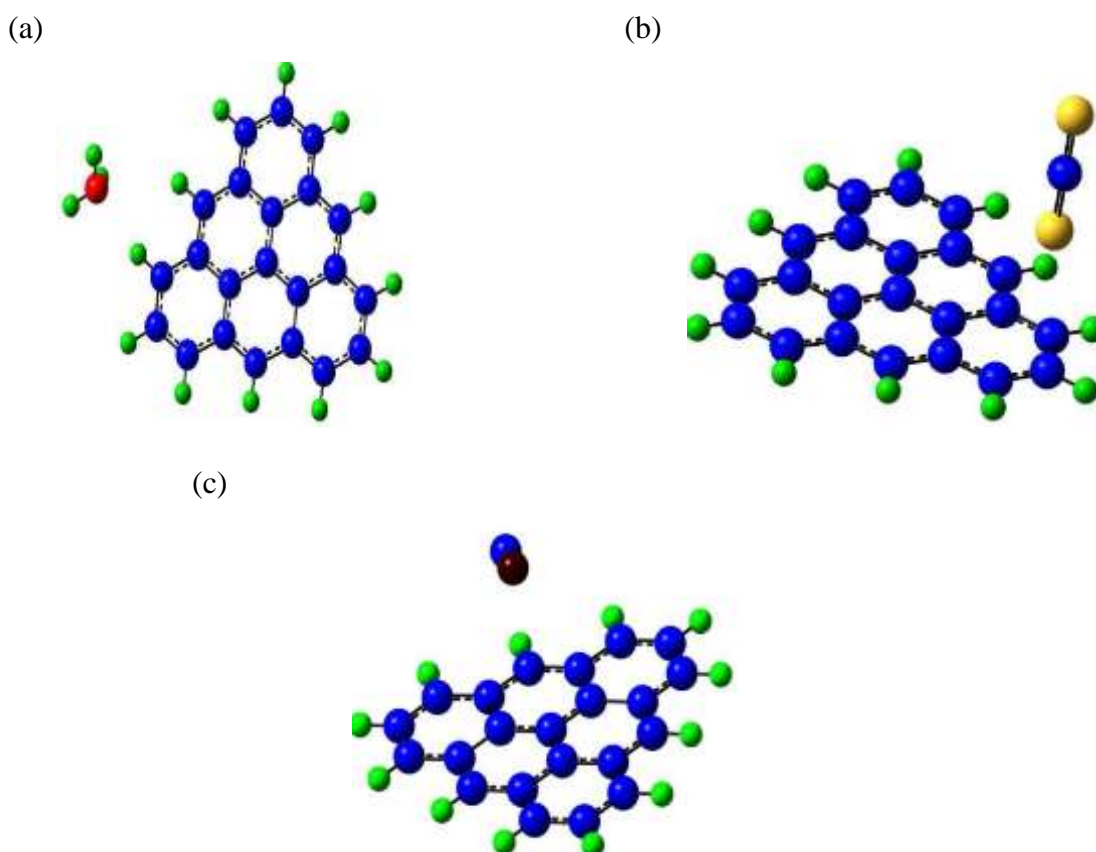


Figure-3: Minimum energetic optimized geometry of (a) NH_3 , (b) CS_2 , and (c) CO adsorbed triangulene pristine, respectively.

- **Electronic properties of CO, CS₂, and NH₃ adsorbed Triangulene:**

The charge transfer upon adsorption of gas molecules on triangulene is analysed based on Muliken charge population analysis with the same level of theory and basis set. After adsorption of gas molecules charge transfer is taken place from adsorbate to adsorbent. The Muliken population analysis is shown in Fig.4. Another important parameter is the electric dipole moment vector which shows the charge distribution of a system is also calculated. The dipole moment for pristine triangulene is 4.63 D(Debye). After adsorbing CO, CS₂, and NH₃ gas molecules, its dipole moment becomes 4.99D, 5.29D, and 7.47 D, respectively [5]. To obtain a better understanding about the interaction between gas molecules and triangulene, HOMO and LUMO are calculated. After the adsorption of gas molecules HOMO-LUMO energy gap of triangulene, Fig 5.

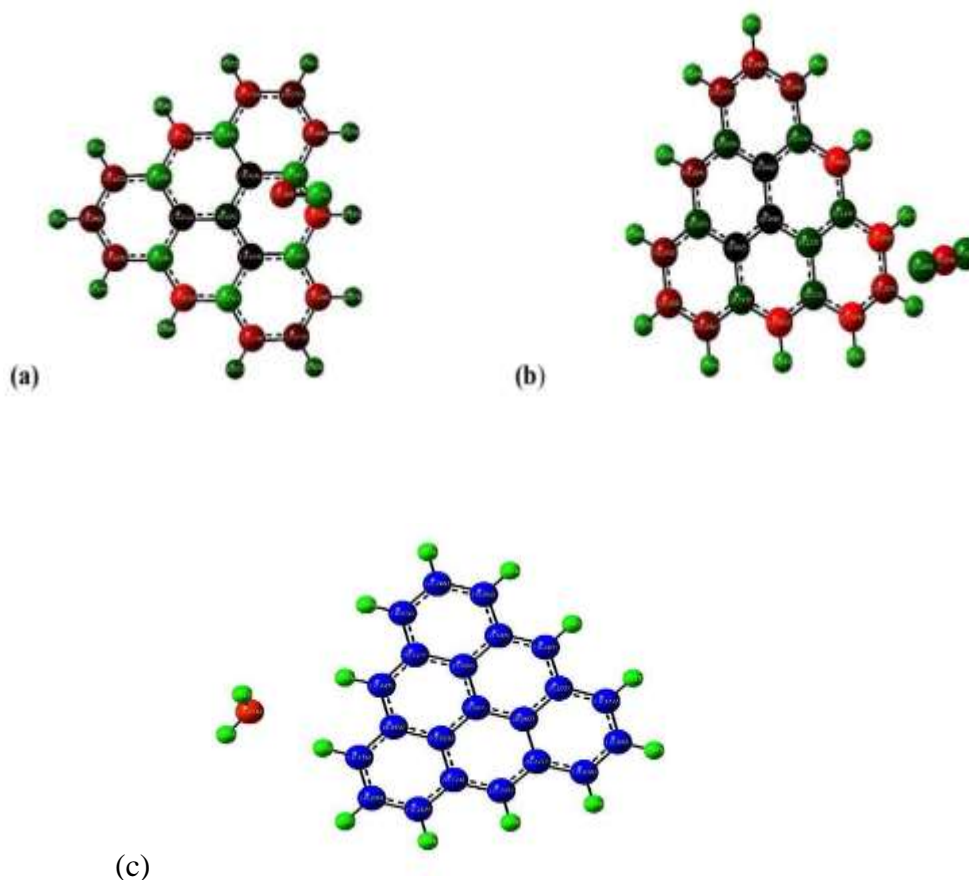


Figure.4: Muliken charge population analysis of (a)CO (b)CS₂ (c)NH₃ gas adsorbed on pristine triangulene.

(a)

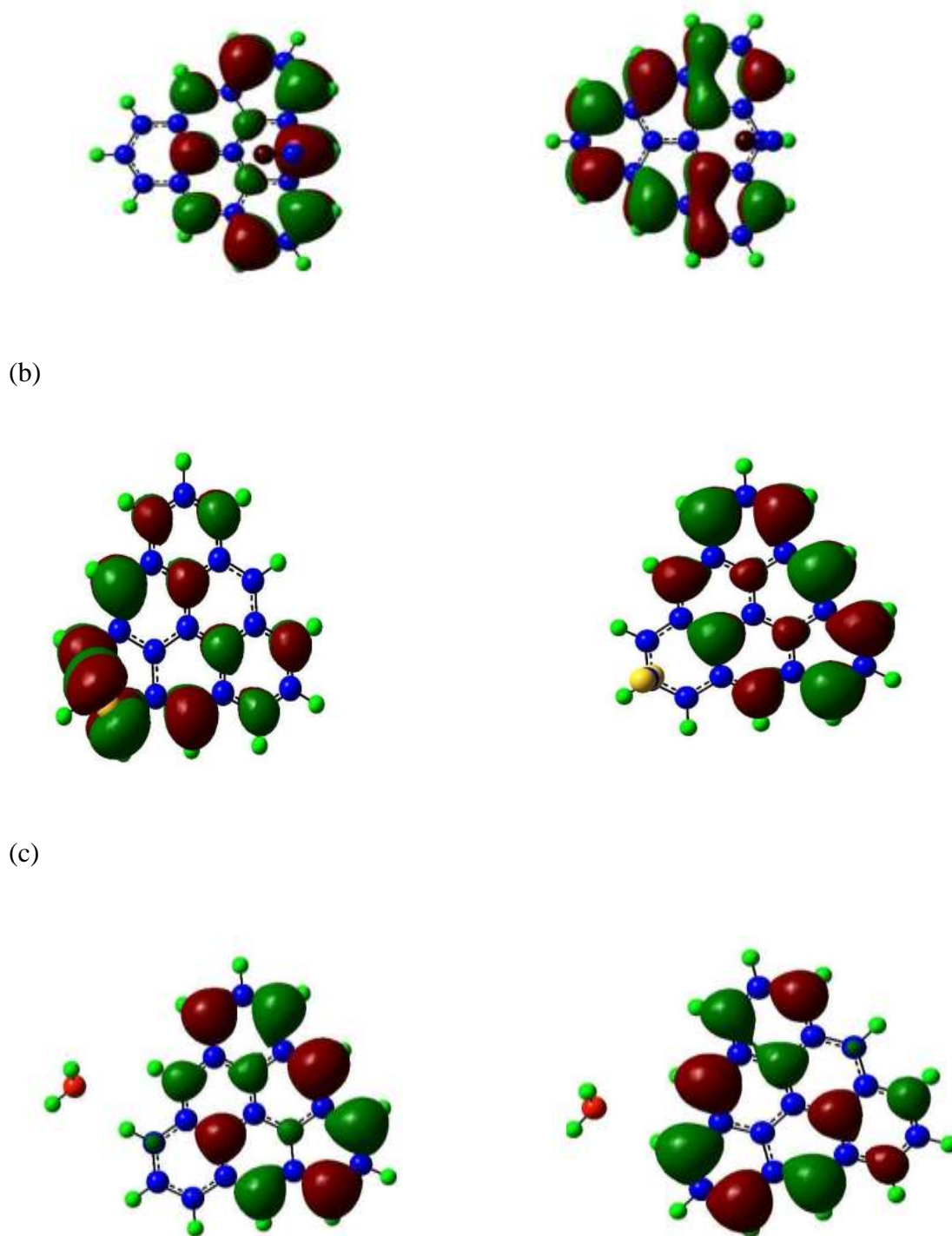


Figure 5: HOMO and LUMO electron density of (a)CO (b)CS₂ (c)NH₃ gas molecules adsorbed triangulene.

We analysed the density of state for gas molecules adsorbed triangulene pristine, as shown in Fig.6. the calculated fermi energy level E_f (using eq (2)) which is -3.53eV, -3.58eV and - 3.27eV, for CO, CS₂ and NH₃ gas molecules adsorbed triangulene, respectively

(a)

(b)

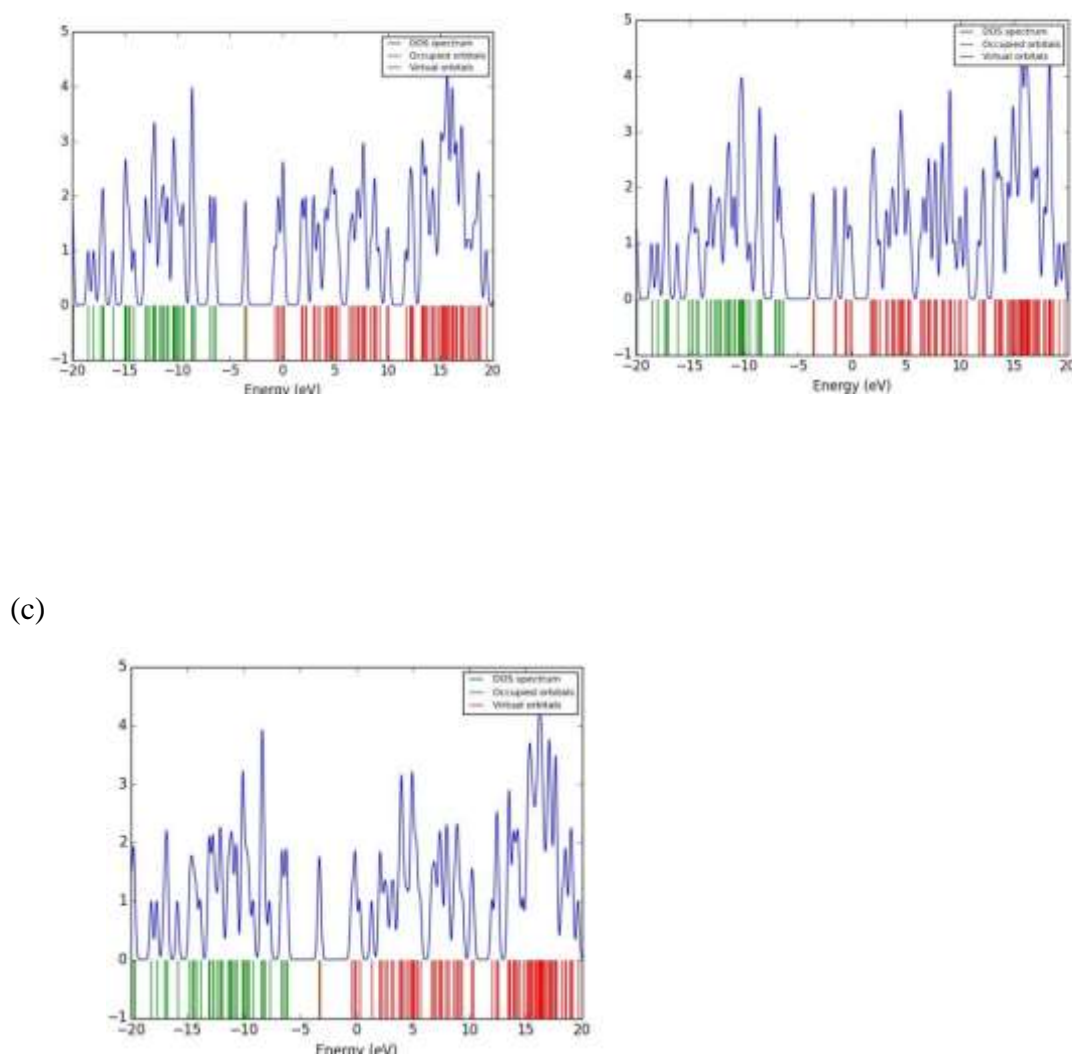


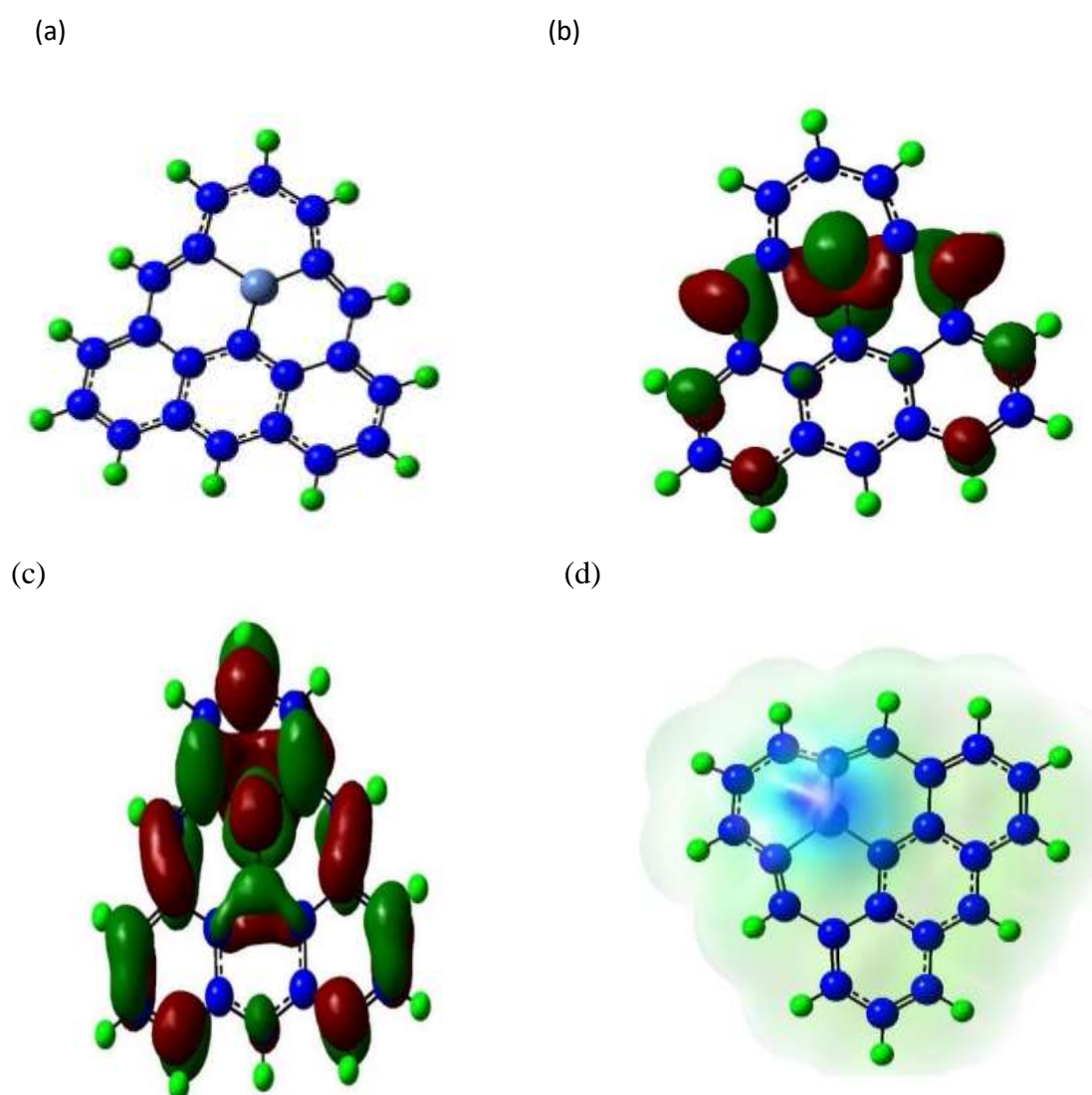
Figure 6: DOS spectra of (a)CO (b)CS₂ (c)NH₃ gas molecules adsorbed triangulene.

Here, Pristine Triangulene shows poor adsorption performance towards CO, CS₂ and NH₃ gas. That's why We are going to use doping mechanism with transition metal (Ni), in order to enhance the gas adsorption performance.

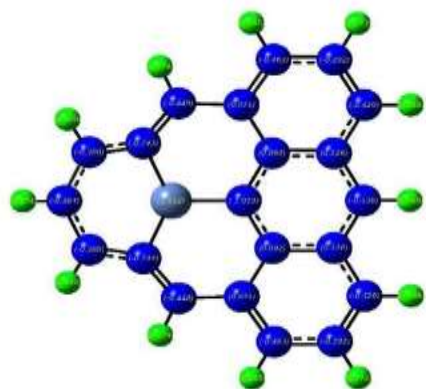
• Structural and electronic properties of Ni-doped Triangulene:

The optimized structure of Ni doped triangulene GQD (C₂₁NiH₁₂) can be shown in fig 7(a). Which is optimized same basis set and functional group which is stated above in case of pristine. The Ni doped Triangulene contains 21 carbon atoms, one Ni atom and 12 Hydrogen atoms. The highest occupied molecular orbital (HOMO) and lowest unoccupied molecular orbital (LUMO) energies in case of C₂₁NiH₁₂ are -4.75eV and -2.30eV respectively. The HOMO – LUMO energy gap is calculated using eq (3) and the value is 2.45eV and corresponding Fermi energy is calculated using eq(4) and the value is -3.52eV which is lies exactly middle of HOMO and LUMO energies. In

HOMO – LUMO and ESP maps(see fig.7 (b,c,d)) colour choice is arbitrary, red and green colour represents the negative and positive isosurface respectively. From ESP analysis we can identify which site of system is more suitable for adsorbing gas molecules [6]. To understand the charge distribution of the C₂₁NiH₁₂ GQD, we have analysed Muliken charge population which clearly shows that the positive and negative charge distribution on adjacent carbon atoms and hydrogen atoms respectively (see fig. 7(e)). Fig. 7(f) presents the density of states (DOS) plot of the Ni doped triangulene which collaborate the calculated value of HOMO, LUMO, and E_G as shown in table 4.



(e)



(f)

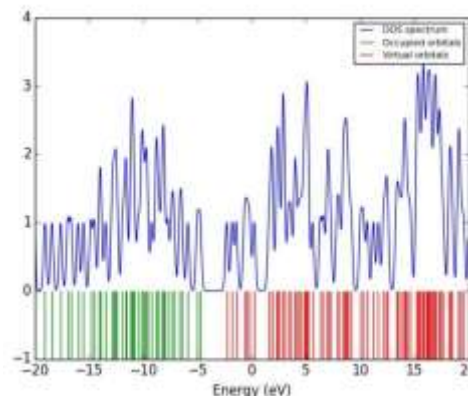


Figure-7 (a) optimized geometry, (b) HOMO electron density, (c) LUMO electron density, (d)ESP, (e) Muliken charge population analysis, (f) dos spectrum of Ni doped triangulene, respectively.

system	Bond Length(Å)	Bond Angle (°)	E _{HOMO} (eV)	E _{LUMO} (eV)	E _G (eV)	DIPOLE MOMENT (DEBYE)	E _f (eV)
Ni doped triangulene	1.79	99.72	-4.75	-2.30	2.45	1.07	-3.52

Table-4: Structural parameter, HOMO and LUMO energies (E_{HOMO} and E_{LUMO}), HOMO LUMO band gap (E_G) and dipole moment of Ni doped triangulene.

To confirm the structural stability of Ni dope triangulene the formation of energy is calculated by the following formula

$$E = (1/34) [E(C_{21}NiH_{12}) - 21E(C) - 12E(H) - E(Ni)] \text{-----(13)}$$

Where, E(C₂₁NiH₁₂) the energy of Ni dope triangulene, E(C) is the energy of the isolated carbon, E(H) is the energy of the isolated hydrogen and E(Ni) is the energy of Ni atom, respectively. The formation energy of Ni dope triangulene is -6.65eV/atom. The negative value of the formation energy ensures the stability of the triangulene.

● Adsorption properties of CO, CS₂ and NH₃ gas molecules adsorbed C₂₁NiH₁₂ GQD:

We have already optimized the isolated hazardous gas molecules (CO, CS₂ and NH₃), analysed structural and vibrational properties. The interaction of the gas molecules with Ni doped triangulene can be understood by adsorption energy, E_{ad} and it is calculated using the formula:

$$E_{ad} = E(C_{21}NiH_{12} + \text{Gas}) - E(C_{21}NiH_{12}) - E(\text{Gas}) \text{-----(14)}$$

where $E(C_{21}NiH_{12} + Gas)$, $E(C_{21}NiH_{12})$ and $E(Gas)$ are the total energy of gas adsorbed Ni doped triangulene, total energy of Ni doped Triangulene and total energy of isolated gas molecule, respectively. We have adsorbed hazardous gas molecules CO, CS₂ and NH₃ at various sites of C₂₁NiH₁₂ GQD and various orientations of the gas molecules at each site of Ni doped Triangulene. The computed adsorption energy (using eq (14)) of CO gas molecules over C₂₁NiH₁₂ is -0.97eV . Fig 8(a) shows minimum energetic configuration for CO absorption. Which clearly shows that CO adsorbed via chemisorption. After CO gas adsorption, adsorption distance change from 2.00 \AA to 1.85 \AA . The adsorption energy (using eq (14)) of CS₂ gas molecules over C₂₁NiH₁₂ is -0.52 eV . Fig 8(b) shows minimum energetic configuration for CS₂ absorption. Which clearly shows that CS₂ adsorbed via chemisorption. After CS₂ gas adsorption, adsorption distance change from 2.00 \AA to 2.24 \AA . The adsorption energy (using eq (14)) of NH₃ gas molecules over C₂₁NiH₁₂ is -1.23eV . Fig 8(c) shows minimum energetic configuration for NH₃ absorption. Which clearly shows that NH₃ adsorbed via chemisorption. After NH₃ gas adsorption, adsorption distance change from 2.00 \AA to 2.05 \AA .

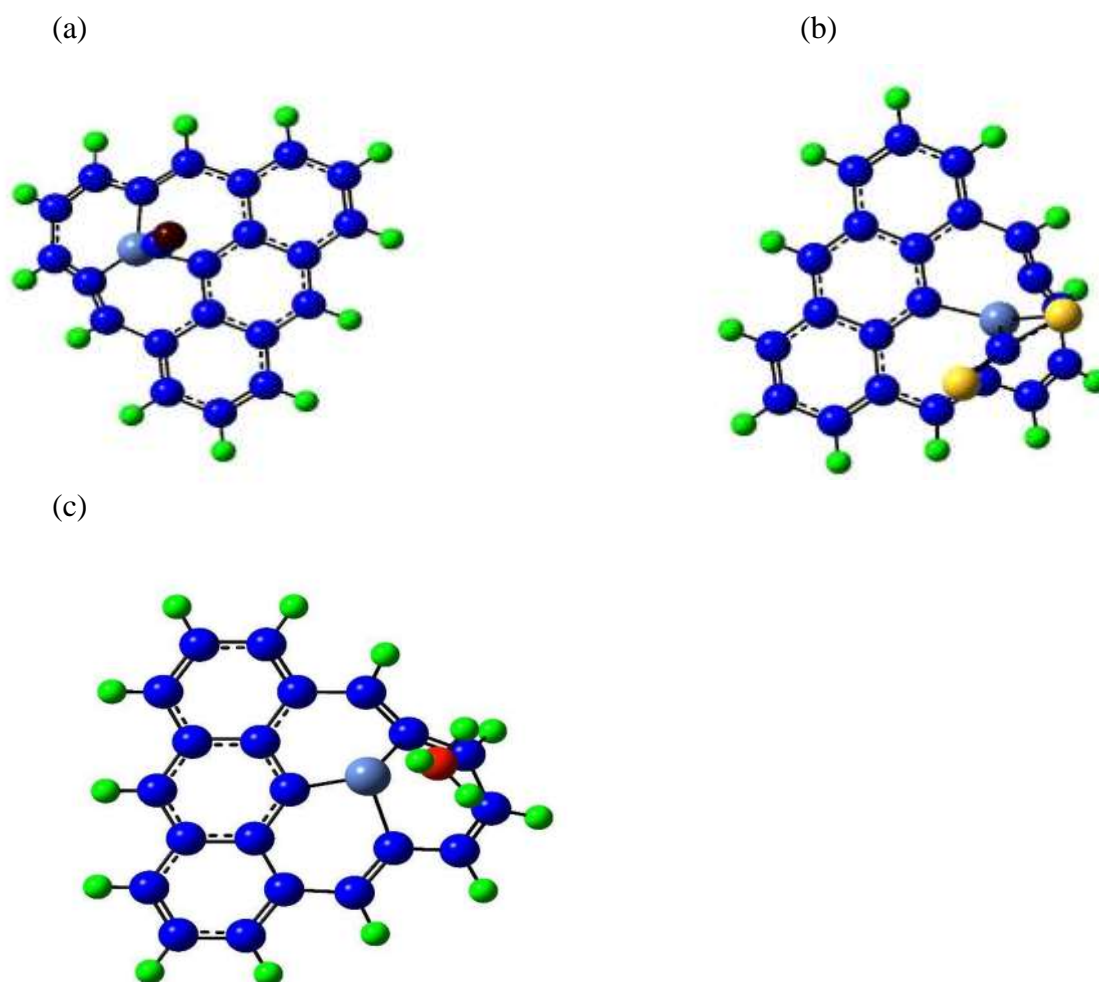
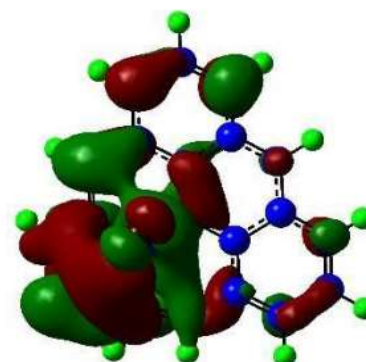
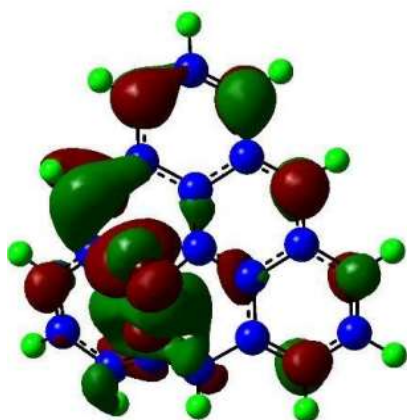


Figure-8: Minimum energetic optimized geometry of (a) CO, (b) CS₂, and (c) NH₃ adsorbed Ni doped triangulene, respectively.

- **Electronic Properties of CO, CS₂ and NH₃ adsorbed C₂₁NiH₁₂ GQD:**

Due to interaction between gas molecules and C₂₁NiH₁₂ GQD there is always a possibilities of charge transfer. The charge transfer is analysed using Mullikan charge population. After CO, CS₂ and NH₃ adsorption, total Mullikan charge on the gas molecules is +0.017e, -0.057e and +0.25e, respectively. This suggests that the charge transfer is taking place from C₂₁NiH₁₂ GQD to CS₂ gas molecules. In the case of CO and NH₃ gas molecule absorption charge transfer is taking from gas molecule to Ni doped triangulene. Because isolated gas molecule CO, CS₂ and NH₃ has total Mullikan charge is zero. The charge distribution of the gas adsorbed C₂₁NiH₁₂ GQD is shown in the Figure 7(e). Furthermore, the electric dipole moment vector, which gives insight into the charge distribution. Due to equal distribution of the charge of the pristine C₂₂H₁₂ GQD, the dipole moment is 4.63 Debye. After substitutional doping of Ni in pristine triangulene, there exist s dipole moment (1.07 Debye) due to Ni atom change charge distribution of triangulene. After adsorbing CO, CS₂ and NH₃ gas molecules, dipole moment changes 0.62 Debye, 3.46 Debye and 5.13 Debye, respectively as shown in table 5. To obtain a deep insight into interaction between gas molecules and C₂₁NiH₁₂, we have calculated the E_{HOMO}, E_{LUMO}, E_F, ΔE_F, E_G and ΔE_G, which are listed in Table 5.[7] We have also analysed the density of states for gas molecules adsorbed C₂₁NiH₁₂ GQD. After CO, CS₂ and NH₃ gas adsorption E_G increased by -13.46%, +8.57% and +10.61%, respectively. the DOS spectrum of CO, CS₂ and NH₃ adsorbed C₂₁NiH₁₂ as shown in Figure 10(a, b, c). From the DOS spectra and Table 3, one can observe the change in Fermi energy and consequent shifting in the corresponding Fermi level. After CO and CS₂ adsorption, the Fermi energy decreases by 7.51% and 4.39% respectively. Furthermore, NH₃ adsorption, Fermi energy increases by 12.62%. Figures 9(a, b, c) present HOMO and LUMO electron densities after CO, CS₂ and NH₃ adsorption over C₂₁NiH₁₂ GQD Respectively, which clearly show the localization of the HOMO electron density between the gas molecule and Ni- doped triangulene and localization of the LUMO electron density between nearest gas adsorbed carbon of C₂₁NiH₁₂ and its neighbouring carbon atom.

(a)



(b)

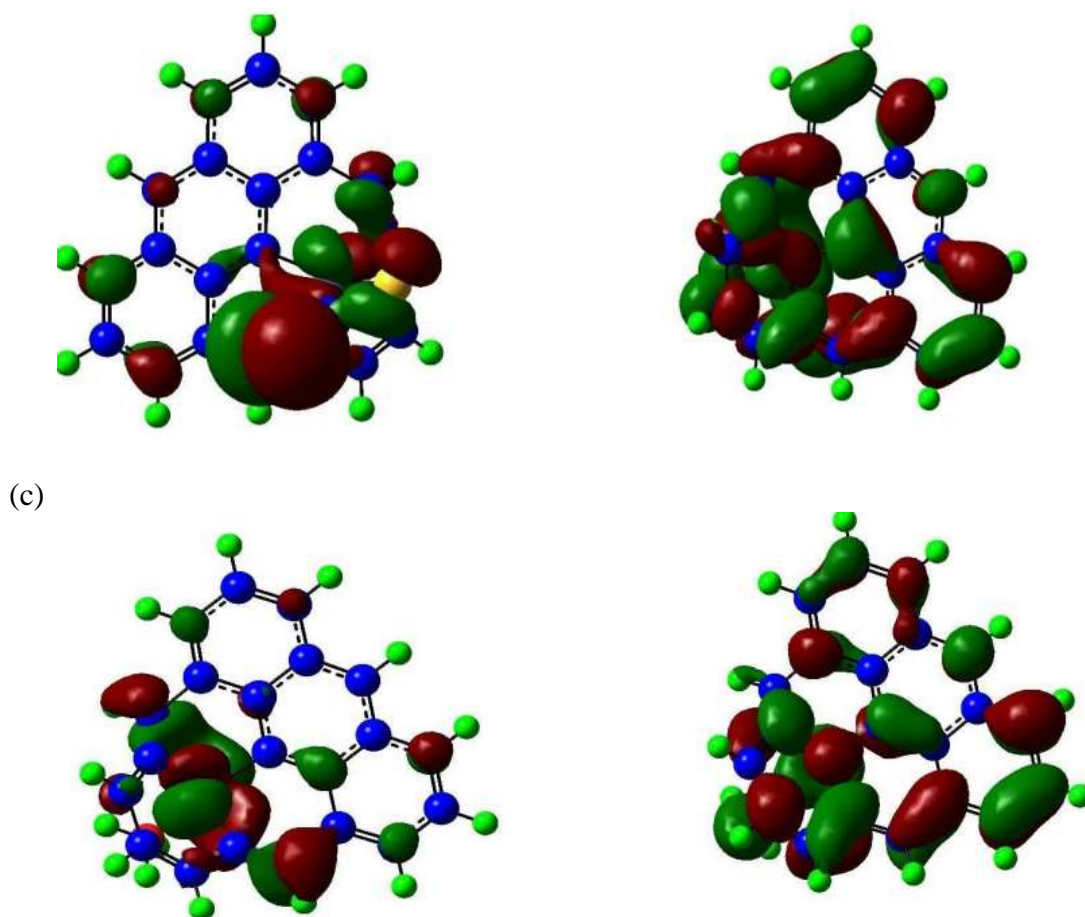
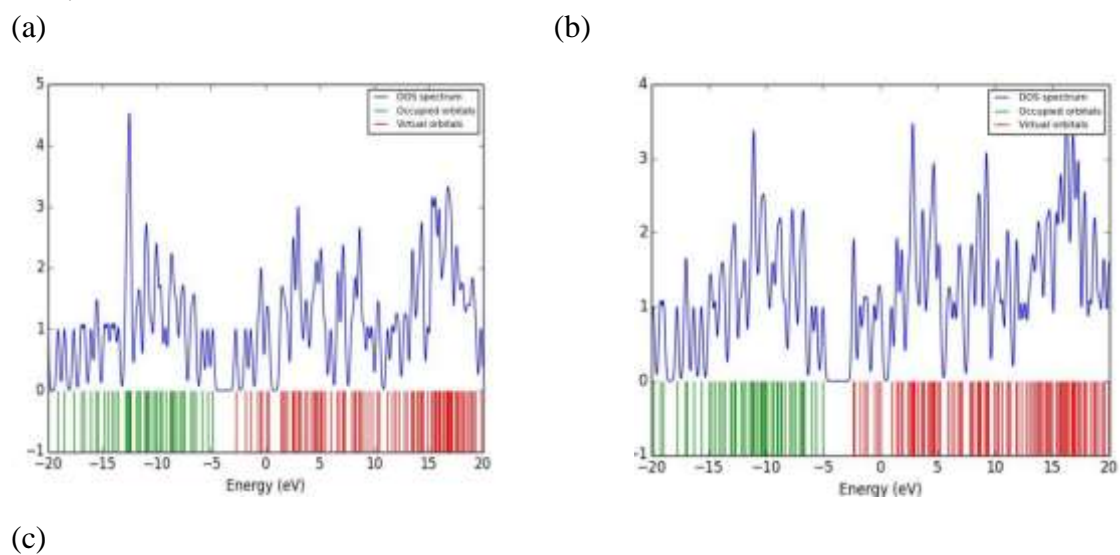


Figure 9: HOMO and LUMO electron density of (a)CO (b)CS₂ (c)NH₃ gas molecules adsorbed Ni doped triangulene



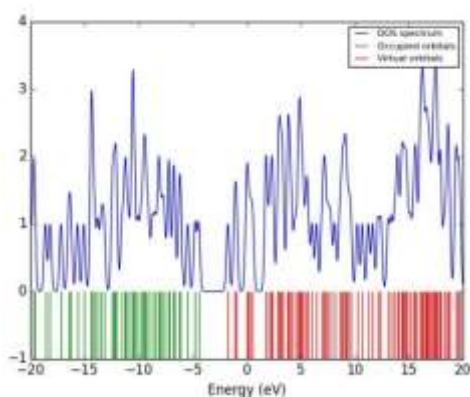


Figure 10: DOS spectra of (a)CO (b)CS₂ (c)NH₃ gas molecules adsorbed Ni triangulene.

System	E _{ads} (eV)	E _{HOMO} (eV)	E _{LUMO} (eV)	E _G (eV)	E _f (eV)	ΔE _f (eV)	ΔE _g (eV)	d(Å)	Dipole Moment (Debye)
C ₂₁ NiH ₁₂ CO	-0.97	-4.85	-2.73	2.12	-3.79	-7.51%	-13.46%	1.85	0.62
C ₂₁ NiH ₁₂ CS ₂	-0.52	-5.01	-2.35	2.66	-3.68	-4.39%	+8.57%	2.24	3.46
C ₂₁ NiH ₁₂ NH ₃	-1.23	-4.44	-1.73	2.71	-3.08	+12.62%	+10.61%	2.05	5.13

Table 5: Adsorption energy (E_{ad}), HOMO energy (E_{HOMO}), LUMO energy (E_{LUMO}), HOMO – LUMO gap (E_G) and fermi energy (E_f) of CO, CS₂ and NH₃ gas adsorbed Ni doped triangulene.

● Sensing properties of C₂₁NiH₁₂ GQD:

The sensing properties of triangulene can be predicted by studying the conductivity given by the following formula

$$\sigma \propto \exp(-E_G/2kT) \text{----- (15)}$$

where σ is the electric conductivity, k is the Boltzmann constant, T is the Kelvin temperature and E_G is the energy gap. According to the eq (15), the electrical conductivity at a given temperature increases with the decrease of energy gap. According to our calculations, we found that the E_G of the pristine triangulene significantly changes with the adsorption of NH₃ and CO. However, E_G does not change much for the adsorption of CS₂ molecules on triangulene pristine. The effective interaction dramatically changes the electronic properties of the triangulene, which in turn help the sensing process.[8] The sensitivity of the triangulene towards CO and NH₃ gas molecules are quite poor (see in table 6). Relative change in conductivity gives sensing response of given system. Which is purely depend on change in HOMO - LUMO gap at constant temperature (here we take room temperature, $T = 300$ K) The sensing response is calculated by formula given below,

$$S = \exp(\Delta E_g / 2KT) - 1 \text{-----(16)}$$

Where ΔE_g is change in HOMO – LUMO gap, K is Boltzmann constant and T is temperature respectively. We can see sensing response of CO , CS_2 and NH_3 gas molecules adsorbed $\text{C}_{21}\text{NiH}_{12}$ in table 6. One of the good characteristics of a chemical sensor is a short recovery time. A strong interaction between the adsorbate and adsorbent molecule is not suitable for a chemical gas sensor because the desorption process will be difficult and the gas sensor will require longer time to recover, and hence recovery time will be greater. The recovery time is calculated with the help of the following equation

$$\tau \propto \vartheta^{-1} \exp(-E_{\text{Ads}}/KT) \text{-----}(17)$$

where E_{Ads} is the adsorption energy, k is the Boltzmann's constant and T is the temperature.[9] As we can see from the equation, the recovery time at a given frequency and temperature increases with the decrease of adsorption energy. For ultra-violet light ($\vartheta \sim 10^{12}\text{s}^{-1}$), the recovery time (in sec) for $\text{C}_{21}\text{NiH}_{12}\text{CO}$, $\text{C}_{21}\text{NiH}_{12}\text{CS}_2$, $\text{C}_{21}\text{NiH}_{12}\text{NH}_3$ are 1.56×10^{-4} , 4.08×10^{-4} , 3.42×10^{-8} respectively. These results show that $\text{C}_{21}\text{NiH}_{12}\text{CS}_2$ has relatively short recovery time than $\text{C}_{21}\text{NiH}_{12}\text{NH}_3$ and $\text{C}_{21}\text{NiH}_{12}\text{CO}$. The unusually large recovery time for $\text{C}_{21}\text{NiH}_{12}\text{NH}_3$ reflects the chemisorption occurred in NH_3 adsorbed $\text{C}_{21}\text{NiH}_{12}$.

system	Sensing response	Recovery time(sec)	ϕ (eV)	$\Delta\phi$ (eV)
$\text{C}_{21}\text{NiH}_{12}\text{CO}$	1.038×10^5	1.56×10^{-4}	3.79	+8.28%
$\text{C}_{21}\text{NiH}_{12}\text{CS}_2$	1.024×10^5	4.08×10^{-4}	3.68	+5.14%
$\text{C}_{21}\text{NiH}_{12}\text{NH}_3$	1.030×10^5	3.42×10^{-8}	3.08	-12%

Table 6: calculated sensing response, recovery time and work function.

The work function (f) is defined as the minimum amount of energy required to remove an electron from a material to a point in the vacuum immediately outside the solid surface and given by following equation

$$\phi = V_{\text{el}(+\alpha)} - E_{\text{F}} \text{-----}(18)$$

where $V_{\text{el}(+\alpha)}$ and E_{F} are electrostatic potential energy far from material surface and Fermi energy respectively.[10],[11] From above equation, if $V_{\text{el}(+\alpha)} = 0$, we can write $\phi = -E_{\text{F}}$. The variation in the value of f of an adsorbent system during gas adsorption process changes its field emission characteristics which can be correlated using a classical Richardson-Dushman equation The current density of emitted electron in vacuum is given by Richardson-Dushman equation

$$j = AT^2 \exp(-\phi/KT) \text{-----}(19)$$

where A is the Richardson constant (A/m^2) and T is temperature. The value of ϕ and $\Delta\phi$ as shown in table 6.

❖ CONCLUSION

The pristine triangulene does not show appreciable adsorption towards any hazardous gas molecule. The most appreciable adsorption energy being -0.177eV for NH_3 gas molecule that is why doping is necessary. The negative formation energy and absence on imaginary in the IR spectrum indicated structure and dynamical stability of NI doped triangulene. The recovery time of CS_2 molecule is very low (4.08×10^{-4}) sec that means it can be used as detection purpose. Due to the high adsorption energy (-0.97 eV and -1.23 eV), recovery time (1.56×10^{-4} and 3.42×10^{-8}) sec and shorter adsorption distance (1.85 and 2.05) Å respectively, NI doped triangulene can be used as a remover purpose of CO and NH_3 from specific environments. Despite of the adsorption distance (2.24Å), Ni-doped triangulene can be used for detection of CS_2 gas molecule due to the short recovery time.

• References:

- 1) Abhinaya K, Karthikaikumar S, Sudha K, Sundharamurthi S, Elangovan A, Kalimuthu P. synergistic effect of 9-(pyrrolidine-1-yl) perylene-3,4-dicarboximide functionalization of amino graphene on photocatalytic hydrogen generation. *Sol Energy Mater Sol Cells* 2018; 185:431. <https://doi.org/10.1016/j.solmat.2018.05.045>
- 2) Shen J, Zhu Y, Yang X, Li C. Graphene quantum dots: emergent nanolights for bioimaging, sensors, catalysis and photovoltaic devices, *Chem Commun* 2012;48: 3686. <https://doi.org/10.1039/c2cc00110a>.
- 3) Qian ZS, Shan XY, Chai LJ, Ma JJ, Chen JR, Feng H. A universal fluorescence sensing strategy based on biocompatible graphene quantum dots and graphene oxide for the detection of DNA. *Nanoscale* 2014; 6:5671-4. <https://doi.org/10.1039/c3nr06583a>.
- 4) 17) R. Bhuvaneshwari, R. Chandiramouli, DFT investigation on the adsorption behavior of dimethyl and trimethyl amine molecules on borophene nanotube, *Chemical Physics Letters* 701 (2018) 34– 42.
- 5) Md. Arafat Hossain, Md. Rakib Hossain, Md. Kamal Hossain, Jahirul Islam Khandaker, Farid Ahmed, Tahmina Ferdous, Md. Abul Hossain for an ab-initio Study of the B35 Boron Nanocluster for Application as Atmospheric Gas (NO , NO_2 , N_2O , NH_3) Sensor.
- 6) Shardul Vadalkar, Darshil Chodvadiya, Narayan N. Som, Keyur N. Vyas, Prafulla K. Jha, and Brahmananda Chakraborty for An Ab-initio Study of the C18 nanocluster for Hazardous Gas Sensor Application doi.org/10.1002/slct.202103874.
- 7) R. Newhook and M.E. Meek, Existing Substances Division, Health Canada, Ottawa, Ontario, Canada; and D. Caldbick, Commercial Chemicals Evaluation Branch, Environment Canada, Hull, Quebec by Concise International Chemical Assessment Document 46
- 8) R. Bhuvaneshwari, R. Chandiramouli, DFT investigation on the adsorption behavior of dimethyl and trimethyl amine molecules on borophene nanotube, *Chemical Physics Letters* 701 (2018) 34– 42.

9) Md. Arafat Hossain, Md. Rakib Hos sai2 , Md. Kamal Hossain , Jahirul Islam Khandaker , Farid Ahmed , Tahmina Ferdous , Md. Abul Hossain for an ab-initio Study of the B35 Boron Nanocluster for Application as Atmospheric Gas (NO, NO₂, N₂O, NH₃) Sensor .

10) M. A. Hossain, M. R. Hossain, M. K. Hossain, J. I. Khandaker, F. Ahmed, T. Ferdous, M. A. Hossain, Chem. Phys. Lett. 2020, 754, 137701.

11) Y. Liu, C. Liu, A. Kumar, Mol. Phys. 2020, 118, 1–8.